

Baltic Astronomy, vol. 22, 53-65, 2013

INVESTIGATION OF THE EARTH IONOSPHERE USING THE RADIO EMISSION OF PULSARS

O.M. Ulyanov, A.I. Shevtsova, D.V. Mukha, A.A. Seredkina

*Department of Astrophysics, Institute of Radio Astronomy of NAS of Ukraine,
Krasnoznamennaya str. 4, Kharkov 61002, Ukraine; oulyanov@rian.kharkov.ua*

Received: 2012 November 13; accepted: 2012 November 28

Abstract. The investigation of the Earth ionosphere both in a quiet and a disturbed states is still desirable. Despite recent progress in its modeling and in estimating the electron concentration along the line of sight by GPS signals, the impact of the disturbed ionosphere and magnetic field on the wave propagation still remains not sufficiently understood. This is due to lack of information on the polarization of GPS signals, and due to poorly conditioned models of the ionosphere at high altitudes and strong perturbations. In this article we consider a possibility of using the data of pulsar radio emission, along with the traditional GPS system data, for the vertical and oblique sounding of the ionosphere. This approach also allows to monitor parameters of the propagation medium, such as the dispersion measure and the rotation measure using changes of the polarization between pulses. By using a selected pulsar constellation it is possible to increase the number of directions in which parameters of the ionosphere and the magnetic field can be estimated.

Key words: ISM: Earth: ionosphere - techniques: radio astronomy - stars: pulsars

1. INTRODUCTION

The observable radio pulses are generated in the space surrounding a neutron star, which is usually called the pulsar magnetosphere. These radio pulses have a number of specific features, but for using them as sounds of the propagation medium it is essential for them to possess a broadband spectrum, strictly periodic pulse signals and a polarized radio emission. The spectrum of radio pulses of pulsars extends from the decameter to the millimeter ranges, their periods are from milliseconds to seconds, and the degree of linear polarization of the strongest pulses is close to 100%. These three factors make it possible to use the strongest pulses to sound the propagation medium, including the Earth ionosphere.

The aim of this work is to use a polarized periodic pulsar radiation for sounding the Earth ionosphere. In this case, the pulsar emission will be used as an additional source for sounding the ionosphere to monitor rapid fluctuations of the Earth magnetic field along the line of sight.

To solve this problem in a general case of elliptically polarized radio emission propagating along the line of sight, it is advisable to use the Faraday effect which

causes rotation of the polarization plane of this emission in the presence of a magnetic field component parallel to the line of sight. It will be shown that the evaluation of rapid fluctuations in the magnetic field near the Earth will require the estimates of the rotation measure (hereafter RM) for every single pulse of the pulsar. Then, by checking this parameter and by using a model of the propagation medium, it is possible to obtain estimates of rapid fluctuations of the magnetic field near the Earth, and to find possible deviations of the ionospheric parameters from the average.

2. THE MODEL CONCEPTION OF THE POLARIZED PULSAR RADIO EMISSION

Despite more than a forty-year investigation of the pulsar radio emission (PRE) (Hewish et al. 1968, Pilkington et al. 1968), the mechanism of their coherent radio emission remains unclear (Melrose & Luo 2008). Observational data in different frequency ranges show that radio emission of pulsars is polarized (McKinnon 2009). Typically, the linear polarization dominates (Suleimanova & Pugachev 2002), however, the component with circular polarization is also involved (Melrose 2003).

We have simulated radio pulses with the repetition period corresponding to the rotation period of a pulsar, $P = 1$ s. In order to simulate the most common case considering the presence of both linear and circular polarizations in PRE, we have included the elliptical polarization into the model. The model signal was generated as follows:

(1) First, using a random number generator that provides a uniform distribution of random variables, we generated the carrier frequencies $f(k)$ which were then uniformly distributed in bandwidths. As the central frequency, we accepted the decametric frequencies at 20 MHz and 30 MHz. These frequencies are commonly used in observations on the UTR-2 radio telescope (Ulyanov et al. 2006, 2008, 2012);

(2) A random number generator has formed the first array of amplitudes $A_0(k)$ which had the Rayleigh distribution with the given r.m.s. deviation (σ_1). Each amplitude in the array matched its radio frequency, see Equation (1) below;

(3) The second amplitude array $B_0(k)$, which had a similar distribution but different standard deviation (σ_2), was consistent with the orthogonal (relative to the first array) linearly polarized component of the radiation on the same carrier frequency as in the item (2). The ratio of standard deviations (σ_1/σ_2), taken for the two Rayleigh amplitude distribution laws determined the compression ratio of the ellipse. Commonly, this ratio is considered to be not higher than 0.5;

(4) Similarly, a white noise was generated with a normal distribution and added to the signal. For the greater clarity and more accurate interpretation of the results, we used the signal/noise ratio (S/N) > 20 ;

(5) The amplitude of the set of noise-like carrier frequencies was modulated. The envelope $G(t)$ of the modulated signal had the Gaussian shape with width not exceeding 10% of the pulsar period. Thus, a pulse nature of the pulsar signal was simulated in the observer frame, see Equation (2) below;

(6) We specified a variation of the position angle (PA) along the average profile of the pulse envelope, using a function which is smooth and slowly varying along the pulse profile $\chi(t) = \arctan((t - t_{center})/m)$. The denominator in the argument of this function could be changed, simulating different slope of the PA trend in the pulse window. A similar shape of the PA trend is actually observed in the polarized

radio emission of pulsars in different frequency ranges (Karastergiou and Johnston 2006);

(7) Due to limited resources of the computer, in both ranges (20 MHz and 30 MHz), the bandwidths were chosen to be relatively small and equal to 4.8 kHz;

(8) To simplify the solution of the direct and inverse problems, we used the analytical form for the representation of model signals (Marple 1999).

Thus, two independent channels (A and B) were formed in which the simulated pulse signals had an orthogonal linear polarization and PA of a given trend. The resulting signal possessed a given ellipticity coefficient and a specified (S/N) ratio.

These model concepts of the signal are formed on the assumption that the propagation channels have relatively narrow bands. In addition, we believe that the tested signals have a fixed ellipticity coefficient on the altitudes of the pulsar magnetosphere which are higher from the surface than the critical polarization radius (Petrova 2006a,b). We should also consider the effect of retardation, the effect of aberration, the dispersion delay of signals in a cold plasma, and the Faraday effect in propagation at the altitudes exceeding the critical radius of polarization (Wang et al. 2011). The first two effects are the kinematic ones and, as it was shown by Ulyanov (1990), at the first approximation they compensate each other. The Faraday effect is related to the rotation of the polarization plane along the line of sight. It is caused by different phase propagation velocity of the ordinary (O) and extraordinary (X) waves (Ginzburg 1967) which arise due to different refractive indices of these waves in a cold anisotropic plasma.

The following equations represent the signals themselves. For the index $k \leq N$, where $f(N)$ is the Nyquist frequency, analytic signal is:

$$\begin{aligned}\dot{E}_{0x}(k, t) &= A_0(k) \cdot e^{-i(2\pi f(k)\tau(t))} \\ \dot{E}_{0y}(k, t) &= B_0(k) \cdot e^{-i(2\pi f(k)\tau(t)-\pi/2)} ,\end{aligned}\quad (1)$$

where $A_0(k) = \sqrt{-2\sigma_1 \ln(1 - x(k))}$ and $B_0(k) = \sqrt{-2\sigma_2 \ln(1 - y(k))}$ are the sets of amplitudes for each channel respectively, $x(k)$ and $y(k)$ are the independent random values with uniform distribution from 0 up to 1, $f(k)$ is the set of frequencies, $\tau(t)$ is the time sample. For $k > N$; $\dot{E}_{0x,0y}(k, t) = 0$. Then the signal is summed to the index k , and in the form of an impulse to the presence of noise is written as:

$$\begin{aligned}\dot{E}_x(t) &= G(t) \cdot \sum_k \dot{E}_{0x}(k, t) + N_x(t) \\ \dot{E}_y(t) &= G(t) \cdot \sum_k \dot{E}_{0y}(k, t) + N_y(t) ,\end{aligned}\quad (2)$$

where $G(t)$ is the Gaussian envelope function, $N_{x,y}(t)$ is the white noise.

3. THE MODEL CONCEPTION OF THE PROPAGATION MEDIUM

At this stage of study, the best solution is to present the propagation medium in a form of layers with changable parameters in accordance with the known analytical laws. In this approach, each layer in the propagation medium is convenient to represent by an eikonal equation $\nabla\varphi(\omega) = n(\omega)\vec{k}(\omega)$, where $\varphi(\omega)$ is the signal phase, $n(\omega)$ is the refractive index of the medium, $\vec{k}(\omega)$ is the wave vector. This equation is applicable to the situation when the propagation medium still has no non-linear effects. By using Taylor series expansion of the refractive index $n(\omega)$, in

the presence of the longitudinal component of the magnetic field along the line of sight, it is possible to keep only the first three terms which consider the influence of the propagation medium. These terms are additive.

The key moment when using an eikonal equation for modeling the propagation medium is to present the refractive indices of the ordinary and extraordinary waves (Ginzburg 1967). With the quasi-longitudinal propagation, according to Zheleznyakov (1977, 1997), we define the ordinary wave as a wave which has the right circular polarization while the direction of its wave vector coincides with the direction of the magnetic field vector, and the magnetic field itself is directed to the observer. Accordingly, the extraordinary wave will have the left circular polarization under the same conditions. If the magnetic field is directed from the observer to the source and the wave vector has the opposite direction, the ordinary wave will have the left circular polarization, and the extraordinary wave - the right circular polarization. Now we define the refractive indices in the propagation medium (one of which, $n_O(\omega)$, corresponds to the ordinary wave and another one, $n_X(\omega)$, to the extraordinary wave) by the following equation: $n_{O,X}(\omega) = \sqrt{1 - \omega_p^2/\omega(\omega \mp \omega_H)}$.

Let us consider under which conditions and/or limitations it is fair to use the equations of a quasi-longitudinal propagation. The determining value of the analysis of radio wave modes in the presence of magnetic field is a characteristic $u = (\omega_H/\omega)^2 = (e|\vec{B}|/(m_e c \omega))^2$. For the propagation conditions in the galactic interstellar plasma at the lowest observation frequency of 20 MHz, where the average values of the magnetic induction $\langle |\vec{B}_{ISM}| \rangle \approx 1 \mu G$, the parameter u is equal to $u = 1.96 \cdot 10^{-14}$. Thus it is evident that for all angles between the wave vector \vec{k} and \vec{B}_{ISM} , except of the angles $\angle \vec{k} \vec{B}_{ISM}$ close to $\pm \pi/2$, the propagation of waves at frequencies above 20 MHz has a quasi-longitudinal nature with circular normal modes.

Propagation conditions in the Earth ionosphere should be considered in more detail. To determine the ellipticity of normal modes of the radio emission in a cold anisotropic plasma, we use the following equation (Zheleznyakov 1997):

$$K_{O,X} = \frac{2\sqrt{u} \times \cos(\angle \vec{k} \vec{B}_I)}{u \times \sin^2(\angle \vec{k} \vec{B}_I) \pm \sqrt{u^2 \times \sin^4(\angle \vec{k} \vec{B}_I) + 4u \times \cos^2(\angle \vec{k} \vec{B}_I)}}, \quad (3)$$

where \vec{B}_I is the magnetic induction vector in the Earth ionosphere.

The magnitude and direction of \vec{B}_I which is required for the analysis, depend on the geographical coordinates of the phase center of the receiving radio telescope. All the data from Equation (3) will be given for a mid-latitude radio telescope UTR-2 with the following coordinates: $49^\circ 38' 17.6''$ N, $36^\circ 56' 28.7''$ E, and the altitude 180 m. On the date of observation, the magnetic induction vector in the phase center of UTR-2 had the following parameters $|\vec{B}_I| = 50419 \times 10^{-9}$ T, i.e., about 0.5 G. The vertical and horizontal components had the values $|\vec{B}_{Iv}| = 46311.6 \times 10^{-9}$ T and $|\vec{B}_{Ih}| = 19932.7 \times 10^{-9}$ T, respectively. In this case, the horizontal component of the vector corresponds to the South - North direction with a slight deviation (about 7°) to the East. Thus, the inclination angle of the magnetic induction is about 23° . Since in the first approximation

the Earth magnetic field has a dipole character, the value of its magnetic intensity decreases with height as $|\vec{B}_I| \sim 1/R^3$, where R is the distance from the center of the magnetic dipole (the center of the Earth). Daily variations of the Earth magnetic field for undisturbed conditions at middle latitudes do not exceed $|\delta\vec{B}_I| \leq 50 \cdot 10^{-9}$ T.

Then, by substituting the above parameters to Equation (3), we obtain the values of ellipticity coefficients $K_O = -1/K_X$ for the normal modes of radio emission in the phase center of the UTR-2 radio telescope at any angle between \vec{k} and \vec{B}_I (see Figure 1).

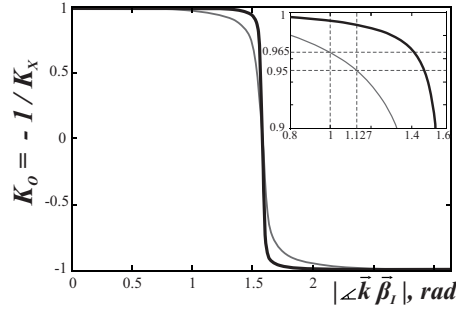


Fig. 1. Ellipticity coefficient for normal modes in the angular range $0 \leq \angle|\vec{k}\vec{B}_I| \leq \pi$ at the frequencies 23.7 MGz (thin line) and 111 MGz (thick line).

From Figure 1 it is evident that in the angular range $0^\circ \leq (\angle\vec{k}\vec{B}_I) \leq 65^\circ \cup 115^\circ \leq (\angle\vec{k}\vec{B}_I) \leq 180^\circ$ both ellipticity coefficients at frequencies $F_c \geq 23.7$ MHz exceed by absolute value the 0.95 level for the considered conditions. Such values of ellipticity coefficients of the normal modes correspond to the case of quasi-longitudinal propagation in a given range of angles at frequencies that exceed the above value. Therefore, the further analysis will be done from the point of view of a quasi-longitudinal propagation with the circular normal modes.

For a transverse wave propagating along the axis z , the eikonal equation is:

$$\frac{d\varphi_{O,X}(\omega)}{dz} = n_{O,X}(\omega)k(\omega) = n_{O,X}(\omega)\frac{\omega}{c}. \quad (4)$$

The expansion of Equation (4) in Taylor series gives the phase of the signal detected in any space-time point on the line of sight:

$$\varphi_{O,X}(\omega) \approx \frac{\omega L}{c} - \frac{1}{\omega} \frac{2\pi e^2}{m_e c} \int_0^L N_e(z) dz \mp \frac{1}{\omega^2} \frac{2\pi e^3}{m_e^2 c^2} \int_0^L N_e(z) |\vec{B}| \cos(\angle\vec{k}\vec{B}) dz, \quad (5)$$

where c is the speed of light, e is the electron charge, m_e is the electron rest mass, L is the distance between a pulsar and an observer or the layer thickness, $N_e(z)$ is the electron concentration at the line of sight, $|\vec{B}| \cos(\angle\vec{k}\vec{B})$ is the magnetic field intensity along the propagation path.

In Equation (5), the terms are grouped so as to separate in the propagation in vacuum, the dispersion delay and the Faraday effect. Equations (6) and (7) show

the phase shift caused by these two effects, respectively:

$$\alpha(DM, \omega) \approx \frac{1}{\omega} \frac{2\pi e^2}{m_e c} \int_0^L N_e(z) dz = \frac{e^2}{m_e c} DM \frac{1}{f}, \quad (6)$$

$$\psi_{O,X}(RM, \omega) \approx \mp \frac{1}{\omega^2} \frac{2\pi e^3}{m^2 c^2} \int_0^L N_e(z) |\vec{B}| \cos(\angle \vec{k} \vec{B}) dz = \mp RM \lambda^2, \quad (7)$$

where $DM = \int_0^L N_e(z) dz$ is the dispersion measure, $f = \omega/(2\pi)$, λ is the wavelength, $RM = \frac{e^3}{2\pi m^2 c^4} \int_0^L N_e(z) |\vec{B}| \cos(\angle \vec{k} \vec{B}) dz$ is the rotation measure.

Now we can move on to the matrix description of the layered model of the propagation medium. The matrices, which are responsible for the dispersion delay in a cold isotropic plasma and for the Faraday rotation in the presence of magnetic field commute. Therefore, the solution of both the direct and the inverse problems is greatly simplified due to a possibility to enter and to offset the impact of these two propagation effects separately. Accordingly, the inverse problem can be solved by using the matrix inversion, used in the construction of the direct problem.

Herein we give the equations in a matrix form for the signals that can be detected by using the so-called Wave Form (WF) receivers (Zakharenko et al. 2007) in a homogeneous layers of the interstellar medium (ISM) and the Earth ionosphere:

$$\begin{bmatrix} \dot{E}_x^{space}(\omega) \\ \dot{E}_y^{space}(\omega) \\ \dot{E}_z^{space}(\omega) \end{bmatrix} = D \times T_{lc}^{-1} \times R \times T_{lc} \times PA \times \begin{bmatrix} \dot{E}_x(\omega) \\ \dot{E}_y(\omega) \\ \dot{E}_z(\omega) \end{bmatrix}, \quad (8)$$

$\dot{E}_{x,y,z}^{space}(\omega)$ are the signals in the free space under ionosphere, $\dot{E}_{x,y}(\omega)$ are created signals from Eq.(2) ($\dot{E}_z(\omega) = 0$), T_{lc} is the transfer matrix from linear basis to circular basis, $T_{lc}^{-1} = T_{cl}$ is the inverse transfer matrix.

$$T_{lc} = \frac{1}{\sqrt{2}} \begin{bmatrix} 1 & i & 0 \\ 1 & -i & 0 \\ 0 & 0 & \sqrt{2} \end{bmatrix}, \quad T_{lc}^{-1} = \frac{1}{\sqrt{2}} \begin{bmatrix} 1 & 1 & 0 \\ -i & i & 0 \\ 0 & 0 & \sqrt{2} \end{bmatrix},$$

$$D = \begin{bmatrix} e^{-i\alpha(DM, \omega)} & 0 & 0 \\ 0 & e^{-i\alpha(DM, \omega)} & 0 \\ 0 & 0 & 1 \end{bmatrix}, \quad R = \begin{bmatrix} e^{i\psi_O(RM, \omega)} & 0 & 0 \\ 0 & e^{i\psi_X(RM, \omega)} & 0 \\ 0 & 0 & 1 \end{bmatrix}$$

are the matrices of phase shifts caused by the dispersion delay and the Faraday effect, $PA = \begin{bmatrix} \cos(\chi(t)) & \sin(\chi(t)) & 0 \\ -\sin(\chi(t)) & \cos(\chi(t)) & 0 \\ 0 & 0 & 1 \end{bmatrix}$ is the rotation matrix with simulated $\chi(t)$.

We should also focus on compensation of the influence of the underlying surface near the interface of two media (air and land) and the redistribution of the intensity of polarization components received by a radio telescope, which appears due to the presence of the underlying surface. So, under $\dot{E}_{x,y,z}^{space}(\omega)$ we mean the corresponding

components of the field at the output of the ionosphere in the plane of the radio telescope phase center that is orthogonal to \vec{k} . Then we extend Equation (8) and take into account the actual ground conductivity by using of the Fresnel reflection coefficients (Eisenberg et al. 1985; Schelkunoff & Friis 1952). These coefficients are different for perpendicular (s) polarization (sticks out of or into the plane of incidence z_0y) and parallel (p) polarization (lies parallel to the plane of incidence) components of the electric field:

$$\dot{\rho}_s = \frac{\cos(\angle z'z) - \sqrt{\dot{\varepsilon} - \sin^2(\angle z'z)}}{\cos(\angle z'z) + \sqrt{\dot{\varepsilon} - \sin^2(\angle z'z)}}, \quad \dot{\rho}_p = \frac{\dot{\varepsilon} \cos(\angle z'z) - \sqrt{\dot{\varepsilon} - \sin^2(\angle z'z)}}{\dot{\varepsilon} \cos(\angle z'z) + \sqrt{\dot{\varepsilon} - \sin^2(\angle z'z)}}.$$

Equation (8), taking into account the underlying surface (we assume that it is flat), is transformed into the following form:

$$\begin{bmatrix} \dot{E}_{x'}^{rec}(\omega) \\ \dot{E}_{y'}^{rec}(\omega) \\ \dot{E}_{z'}^{rec}(\omega) \end{bmatrix} = COS \times (\|1\| + REF) \begin{bmatrix} \dot{E}_x^{space}(\omega) \\ \dot{E}_y^{space}(\omega) \\ \dot{E}_z^{space}(\omega) \end{bmatrix}, \quad (9)$$

where x' ; y' ; z' are the new coordinate axes in the laboratory frame, $\dot{E}_{x',y',z'}^{rec}(\omega)$

are the signals at the receiver, $\|1\| = \begin{bmatrix} 1 & 0 & 0 \\ 0 & 1 & 0 \\ 0 & 0 & 1 \end{bmatrix}$ is the unit matrix (transform

directed signal matrix), $COS = \begin{bmatrix} \cos(\angle x'x) & \cos(\angle x'y) & \cos(x'z) \\ \cos(\angle y'x) & \cos(\angle y'y) & \cos(y'z) \\ \cos(\angle z'x) & \cos(\angle z'y) & \cos(z'z) \end{bmatrix}$ is the ma-
trix of the directional cosines, $REF = \begin{bmatrix} \dot{\rho}_s(\omega, \dot{\varepsilon}, \sigma) \cdot e^{-i\phi} & 0 & 0 \\ 0 & \dot{\rho}_p(\omega, \dot{\varepsilon}, \sigma) \cdot e^{-i\phi} & 0 \\ 0 & 0 & 1 \end{bmatrix}$

is the transform reflected signal matrix, where $\dot{\varepsilon} = \varepsilon_r - i60\sigma\lambda$ is the dielectric index, σ is the conductivity of the underlying surface, $\phi = \omega \frac{2h}{c} \cos(\angle z'z)$ is the phase shift between direct and reflect signals, h is the altitude of the phase center of the dipole.

Finally, the values $\dot{E}_{x,y,z}^{space}(\omega)$ must be set to the laboratory frame of reference, the center of which coincides with the phase center of the telescope, and the axes x', y', z' correspond to directions: phase center-south, phase center-west and phase center-zenith. This is achieved by using the so-called directional cosines matrix (COS) which determines the projection of the transformed components $\dot{E}_{x,y,z}^{space}(\omega)$ to the new axes.

Equation (9) takes into account that the redistribution of the polarization intensities of the incident wave at the receiver site is not only due to the presence of different reflection coefficients, but also due to different path lengths of the incident and reflected waves. From equations (8) and (9) we see the connection between the electrical field vector values at the boundaries of homogeneous layers.

The simplest decision is to compensate for the impact of the dispersion delay as shown in the paper of Hankins (1971). For the coherent compensation of the dispersion delay it is sufficient to multiply the matrix which includes factors of

the dispersion delay by its inverse matrix. Since the matrix, that characterizes this effect in the chosen coordinate basis, is diagonal with a unit determinant, the inverse matrix is simply complex conjugated to the original matrix. This approach allows us to remove the dispersion delay by layers.

Similarly, by using the multiplication to the inverse matrix, the effect of the rotation of the polarization plane is compensated. There is also a possibility of partial or gradual compensation of the Faraday effect.

4. THE METHODS OF THE ANALYSIS

In order to increase the accuracy of the results, we carried out a numerical simulation of the basic processes involved in the generation of the PRE, in the processes of propagation in the cold weakly anisotropic plasma and in the processing of the received signal. For evaluation of the polarization parameters of the received signals, we used a traditional method which uses the polarization tensor (Zheleznyakov 1997). This method requires a relatively long averaging in comparison with the characteristic time of the fluctuations of amplitudes of the field components (Mishchenko et al. 2006). When applied to the pulsar radio emission, the polarization observations are very important as this allows to probe the propagation medium and, in particular, the ionosphere. For the decameter range it is more important to investigate the anomalously strong pulses detected in a number of pulsars (Popov et al. 2006; Ulyanov & Zakharenko 2012).

Since the use of the WF receivers is connected with necessity of storing and processing a huge amount of information, the registration with a parallel spectrum analyzer is mostly used. In this case, the recorded signals contain information on its power spectral density and on the dynamic behavior of the signal envelope.

Hereafter we give the equations which are linking the electric field wave intensity vector with the polarization tensor (Eq. 10) and the Stokes parameters I, Q, U, V (Eq. 11) in a circular and linear cases:

$$J = \begin{bmatrix} I_{xx} & I_{xy} \\ I_{yx} & I_{yy} \end{bmatrix} = \frac{c}{4\pi} \begin{pmatrix} \langle E_x(t) \cdot (E_x^*(t)) \rangle & \langle E_x(t) \cdot E_y^*(t) \rangle \\ \langle E_y(t) \cdot E_x^*(t) \rangle & \langle E_y(t) \cdot E_y^*(t) \rangle \end{pmatrix} , \quad (10)$$

$$\begin{array}{ll} I = I_{rr} + I_{ll} & I = I_{xx} + I_{yy} \\ Q = I_{rl} + I_{lr} & Q = I_{xx} - I_{yy} \\ U = -i(I_{rl} - I_{lr}) & U = I_{xy} + I_{yx} \\ V = I_{rr} - I_{ll} & V = i(I_{yx} - I_{xy}) \end{array} . \quad (11)$$

When these parameters are known, we can determine the polarization degree and PA (Zheleznyakov 1997).

These equations can be used when the received signals are being recorded with a WF receiver. In the case of registering with a spectrum analyzer, we can also recover all the Stokes parameters of the original signal. Then the Faraday effect will cause the polarization ellipse described by the electric intensity vector of the received signal, being projected on a linear vibrator with different position angles for different frequencies. Thus, if in the total band of the reception signal PA of the polarization ellipse makes N turns to π radians, the observer will register the same N periods of radiation intensity modulation in the channel A or B (see Figure 2).

From the above considerations it is evident that the period of the Faraday intensity modulation by the frequency Δf_F corresponds to a phase shift in the position angle $\Delta\psi(RM, f)$ of π radians.

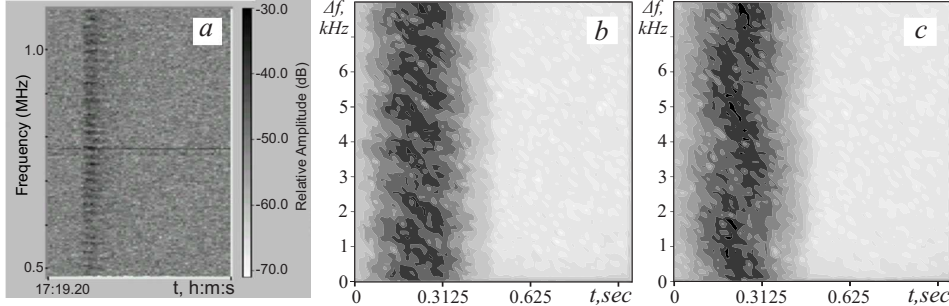


Fig. 2. The dynamic spectra of: a) the elliptically polarized radiation from PSR B0809 +74, detected using UTR-2 ($F_c = 23.7$ MHz, $\Delta F = 1.53$ MHz); b) the model signal ($F_c = 20$ MHz, $\Delta F = 4$ kHz); c) the model signal ($F_c = 30$ MHz, $\Delta F = 4$ kHz).

$$\Delta\psi(RM, f) = c^2 RM \left[\left(\frac{1}{f_c} \right)^2 - \left(\frac{1}{f_c + \Delta f_F} \right)^2 \right], \quad \Delta\psi = \pi \quad . \quad (12)$$

The Faraday modulation intensity period is found from the number n_{max} of the spectral component for which the maximum power response ($|\dot{P}(n_{max}, t)|^2$) is registered. Then the estimate of RM is calculated as:

$$RM = \frac{\pi}{c^2} \left[\frac{f_c^2 (f_c + \Delta f_F)^2}{(f_c + \Delta f_F)^2 - f_c^2} \right] = \frac{\pi}{c^2} \frac{f_c^3}{2\Delta f_F} \quad . \quad (13)$$

The errors of this method in percent are $\delta RM \leq 0.5 \cdot 100/n_{max}$. The phase of the registered spectral component will be linked to PA of the polarization ellipse by the following relation:

$$\chi_{res}(t) = \frac{1}{2} \arg \left(\dot{P}(n_{max}, t) \right) \quad , \quad (14)$$

where $\chi_{res}(t)$ is the PA of the restored signal.

5. THE RESULTS

The above methods were used to construct numerical models of the polarized radio emission of pulsar pulses, as well as for the treatment of three anomalously strong pulses of PSR B0809+74 which were registered with a parallel spectrum analyzer. Figure 2 shows the responses of the broad-band linear vibrators to the modeled radiation pulses of pulsars, which passed through the interstellar medium. These responses (Figure 2, panels b and c) are shown for the receivers with the center frequencies 20 MHz and 30 MHz. The dispersion measure for PSR B0809+74 ($DM = 5.753$ pc/cm³) was introduced into the ISM model, and then removed on the receiving end according to the method described by Hankins (1971) and

Hankins & Rickett (1975). Also, a deliberately high $RM = -234$ rad/m² was introduced in the ISM model. This allowed us to use the narrow-band polarization reception channels without any loss of accuracy. In real observations, the bandwidth of the receiving channels reaches several dozens of MHz what makes it necessary to check the adequacy of the model assumptions in the full bandwidth of the receiver.

Figure 3a shows the Stokes parameters of the model signal in the reference frame connected with the pulsar (dash-dot line) and of the same signal which has passed through the ISM with the given and compensated RM and DM (solid line) parameters. Panel (b) shows the trend of PA which is defined analytically (dashed line) and was restored from the Stokes parameters, derived from the polarization tensor in the solution of the inverse problem.

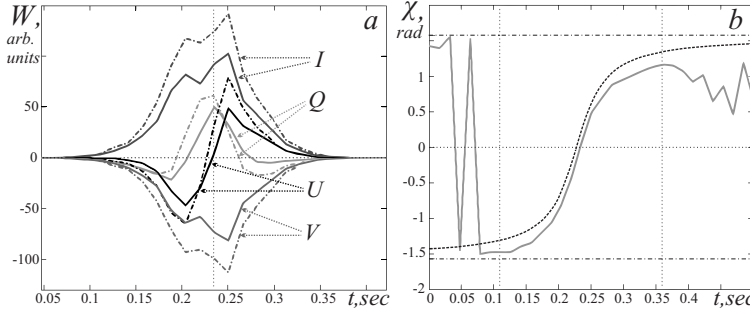


Fig. 3. Panel (a) shows the Stokes parameters and panel (b) - PA calculated from these parameters: $\chi = 1/2 \arg(Q + iU)$.

Three anomalously intensive pulses of PSR B0809+74 that have been registered with the radio telescope UTR-2 and the broad-band linear vibrators, have been processed using the methods described above. In all three cases, the resulting estimate of RM differs from that which was obtained earlier from the high-frequency data, and which we considered to be the aimed parameter of the ATNF catalog (for PSR B0809+74 $RM_{ATNF} = -11.7$ rad/m²). Figure 4 shows the spectral response from which by Equation (13), we obtain RM estimates for each pulse.

The data on the obtained rotation measures and on their determination errors are summarized in Table 1.

Table 1. The rotation measure of the individual pulses of the PSR B0809+74 at the frequency $F_c = 23.7$ MHz.

Pulse	n_{max}	RM_{Est} , rad/m ²	RM_{ATNF} , rad/m ²	ΔRM , rad/m ²	ΔRM , %	δRM , rad/m ²	δRM , %
1 (a)	80	-12.18		-0.48	4.1	0.073	0.625
2 (b)	83	-12.64	-11.7	-0.94	8	0.075	0.602
3 (c)	83	-12.64		-0.94	8	0.075	0.602

In Table 1 the following designations are used: $\Delta RM_{rad/m^2} = RM_{Est} - RM_{ATNF}$; $\delta RM\% = 0.5 \cdot 100/n_{max}$; $\delta RM_{rad/m^2} = \delta RM\% \cdot RM_{ATNF}/100$.

From the results obtained from the variations of the rotation measures for the three individual pulses we conclude that the accuracy of their registering does

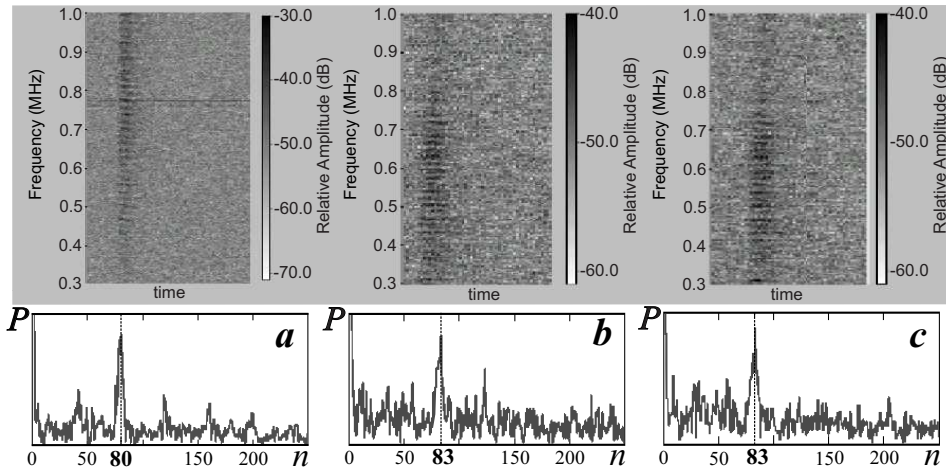


Fig. 4. Top panels. Dynamic spectra of the elliptically polarized radiation of the three anomalously strong pulses of PSR B0809+74 registered with UTR-2 ($F_c = 23.7$ MHz, $\Delta F = 1.53$ MHz). Lower panels. The polarization responses ($P = |\dot{P}(n, t)|^2$) near the maximum intensity of each pulse.

not cause any doubt, since the errors of the method are smaller by an order of magnitude than the variations of RM . Since these variations are registered along the whole way of the radiation from the pulsar to the observer, we should be in caution in their interpretation. In this case, in the reference frame of the observer, the variations were fixed at the time of the dispersion delay of each individual pulse. For the specific observations, this time delay was equal to 5 s. The responsibility for such variations of the RM can carry the variations of the magnetic field and the electron density in the magnetosphere of the pulsar itself, as well as the variations of the same quantities in the Earth ionosphere. In order to distinguish the place of these variations along the line of sight, it is appropriate to lead simultaneous broad-band observations of pulsars, including the high-frequency bands. On the other hand, a comparison of the given data with the two-frequency data obtained from the analysis of the difference between the time of pulse arrival of the GPS system and the same signals of the local hydrogen standards, are needed.

High-frequency data obtained for pulsars, allows us to significantly reduce the time of the dispersion delay, while the two-frequency data comparing the GPS time scales and the hydrogen standards will help us to take into account the variations of electron density in the line of sight in the ionosphere. In general, this will allow us to specify the area of the rapid magnetic field fluctuations along the line of sight. Inclusion in the analysis of a system of many pulsars simultaneously increases the number of directions on which we can study the propagation medium, including the Earth ionosphere. Ultimately, this approach will allow passing to the construction of models of the ionosphere with dynamically varying parameters. This may be resulted in the further development of methods of adaptive radio astronomy described by Afraimovich (1981, 2007).

6. CONCLUSIONS

The layered model of the propagation medium, which can be used together with

the eikonal equation, allows us to split the time delay and the angles of rotation of the polarization plane. Formally, this leads to the appearance of the equations of the commuting matrices, one of which describes the effect of the delay dispersion in a cold plasma, and another one describes the Faraday effect.

Systematic observations of radio pulses of pulsars in the mode of waveform recording or the spectra analyzer mode, together with the data of the dualfrequency GPS monitoring, can more accurately determine the total electron contents in the column of the ionosphere along the line of sight, including the rapid fluctuations of this parameter. Analysis of the polarization parameters derived from these observations allows us to estimate the slow and rapid changes in the magnetic field vector and to include this information to the dynamical model of the ionosphere.

ACKNOWLEDGMENTS. The authors are thankful to Zakharenko V.V. & Deshpande A.A. for their help in the carrying out of the observations. The use of the ATNF databases is acknowledged.

REFERENCES

Afraimovich E. L., 1981, *Astronomy & Astrophysics*, 97, 366
 Afraimovich E. L., 2007, *Rep. of Acad. Science, Moscow*, 417, 818 (in Russian)
 ATNF catalog <http://www.atnf.csiro.au/people/pulsar/psrcat/>
 Eisenberg G. Z, Belousov S.P., Zhurbenko E.M. et al., 1985, *Short-wave antennas*,
 Radio and Communication Publishers, Moscow, 2nd edition (in Russian)
 Ginzburg V. L., 1967, *Propagation of Electromagnetic Waves in Plasmas*, Nauka
 Publishers, Moscow
 Hankins T. H., 1971, *ApJ*, 169, 487
 Hankins T. H., Rickett B. J., 1975, in *Methods in Computational Physics*, vol. 14,
 Radio astronomy, Academic Press, p. 55
 Hewish A., Bell S. J., Pilkington J. D. H. et al., 1968, *Nature*, 217, 709
 Karastergiou A. and Johnston S. 2006, *MNRAS*, 365, 353
 Marple S.L. Jr., 1999, *IEEE Transactions on Signal Processing*, 47, 2600
 McKinnon M.M., 2009, *ApJ*, 692, 459
 Melrose D., 2003, in *Radio Pulsars*, ASPC, 302, 179
 Melrose D., Luo Q., 2008, in *40 Years of Pulsars: Millisecond Pulsars, Magnetars
 and More*, AIPC, 983, 47
 Mishchenko, M.I., Travis, L.D., Lacis, A.A., 2006, *Multiple Scattering of Light by
 Particles*, Cambridge University Press
 Petrova S.A., 2006a, *MNRAS*, 366, 1539
 Petrova S.A., 2006b, *MNRAS*, 368, 1764
 Pilkington J.D.H., Hewish A., Bell S.J., Cole T.W., 1968, *Nature*, 218, 126
 Popov M.V., Kuzmin A.D., Ul'yanov O.M. et al., 2006, *Astr. Rep.*, 50, 562
 Schelkunoff S.A., Friis H. T., 1952, *Antennas: Theory and Practice*, Bell Telephone
 Laboratories, New York : John Wiley & Sons
 Suleimanova S.A., Pugachev V.D., 2002, *Astr. Rep.*, 46, 309
 Ulyanov O.M., 1990, *Kinematics and Physics of Celestial Bodies*, Kiev, 6, 63
 Ul'yanov O.M., Zakharenko V.V., Konovalenko A.A. et al., 2006, *Radio Physics
 and Radio Astronomy* (in Russian), 11, 113
 Ul'yanov O.M., Zakharenko V.V., Bruk Yu.M., 2008, *Astr. Rep.*, 52, 917

Ul'yanov O.M., Zakharenko V.V., 2012, Astr. Rep., 56, 417
Wang C., Han J., Lai D., 2011, MNRAS, 417, 1183
Zakharenko V.V., Nikolaenko V.S., Ulyanov O.M. et al., 2007, Radio Physics and Radio Astronomy (in Russian), 12, 233
Zheleznyakov V.V., 1977, *Electromagnetic Waves in Cosmic Plasma. Generation and Propagation*, Nauka Publishers, Moscow (in Russian)
Zheleznyakov V. V. 1996, *Radiation in Astrophysical Plasmas*, Astrophysics and Space Science Library, vol. 204, Kluwer Academic Publishers, Dordrecht (published in Russian in 1997)